

Towards a Fundamental Understanding of the Stability and Delay of Offline WDM EPONs

Frank Aurzada, Michael Scheutzow, Martin Reisslein, and Martin Maier

Abstract—The fundamental stability limit and packet delay characteristics of offline scheduling, an elementary scheduling mechanism in recently proposed dynamic bandwidth allocation mechanisms for Ethernet passive optical networks (EPONs) with wavelength division multiplexing (WDM), are unknown. For Poisson packet traffic and gated grant sizing, we develop an analytical framework for characterizing the stability limit and packet delay of offline scheduling in WDM EPONs. We consider two reporting strategies: immediate reporting, whereby the report is immediately attached to an upstream data transmission, and synchronized reporting, where all reports are sent at the end of a polling cycle. We find that our analytical framework correctly characterizes the stability limit and approximates the delay of (i) synchronized reporting with arbitrary traffic loading and (ii) immediate reporting with symmetric traffic loading (where the number of equally loaded ONUs is an integer multiple of the number of upstream channels). For immediate reporting with asymmetric traffic loading, we discover and analytically characterize multicycle upstream transmission patterns that may increase or decrease the stability limit from the limit for synchronized reporting. We complement the analysis and simulation for Poisson packet traffic with simulations for self-similar packet traffic and observe that self-similar traffic results in substantially higher delays at low to medium loads as

well as slightly higher stability limits than Poisson traffic.

Index Terms—Delay analysis; Ethernet passive optical network (EPON); Offline scheduling; Stability limit; Wavelength division multiplexing (WDM).

I. INTRODUCTION

Ethernet passive optical networks (EPONs) have recently emerged as an attractive approach for high-speed Internet access. Initial EPON designs considered a single wavelength channel for downstream transmission from the optical line terminal (OLT) to the optical network units (ONUs) and a single channel for the upstream ONU-to-OLT transmissions; see, e.g., [1–12]. However, growing bandwidth demand increasingly motivates research on designs with multiple wavelength channels in each direction using wavelength division multiplexing (WDM); see, for instance, [13–21]. We consider a WDM EPON architecture where each ONU can receive and transmit on any channel, as described in more detail in Subsection II.A.

With *offline scheduling* [22], which is also referred to as *interleaved polling with stop* [11,23], the OLT collects bandwidth requests from all ONUs before making bandwidth allocation and scheduling decisions; see Subsection II.B for details. Offline scheduling is an elementary scheduling technique employed in a number of recently proposed dynamic bandwidth allocation mechanisms for EPONs and WDM EPONs. For instance, most excess bandwidth allocation schemes employ offline scheduling; see, for instance, [1,16,24–26]. Furthermore, a fundamental understanding of the stability and delay characteristics of offline scheduling is important since offline scheduling lies at one of the extreme ends of the online–offline scheduling continuum [22] and is therefore a key benchmark.

EPONs with offline scheduling, and more generally most PONs, have similarities with polling systems (see, e.g., [27,28]) in that the OLT arbitrates the ac-

Manuscript received June 12, 2009; revised November 12, 2009; accepted November 27, 2009; published December 24, 2009 (Doc. ID 112693).

F. Aurzada and M. Scheutzow are with the Institute for Mathematics, Technical University of Berlin, Berlin, Germany.

M. Reisslein (e-mail: reisslein@asu.edu) is with the School of Electrical, Computer, and Energy Engineering, Arizona State University, Goldwater Center, MC 5706, Tempe, Arizona 85287-5706, USA.

M. Maier is with the Institut National de la Recherche Scientifique (INRS), Montréal, Quebec H5A 1K6, Canada.

Digital Object Identifier 10.1364/JOCN.2.000051

cess of the ONUs to the shared upstream wavelength channels. More specifically, the EPON operates in cycles. In a given cycle, the ONUs report their bandwidth demands to the OLT. According to these reports, the OLT grants ONUs upstream transmission windows in the next cycle. With offline scheduling, the OLT waits to receive all reports from a given cycle before assigning grants for the next cycle. The grants are sized depending on the reported bandwidth demands. (We do not consider static periodically recurring grant allocations to the ONUs.) Hence, there is an unused time period equal to the round-trip delay between receiving the end of the last upstream transmission of a cycle at the OLT and receiving the beginning of the first upstream transmission of the next cycle. As a result, the so-called switchover time between serving successive stations is highly dependent on the round-trip time and the traffic generations at the individual ONUs. In contrast, the existing polling models (see, e.g., [27,28]) consider switchover times that are independent of the traffic generation and service. The existing polling system analyses are therefore not applicable to WDM EPONs and despite the elementary nature of offline scheduling in WDM EPONs, the fundamental characteristics of its stability limit and packet delay are unknown.

In this paper, we contribute toward a formal analysis of the fundamental stability and packet delay characteristics of upstream (ONUs-to-OLT) packet traffic in WDM EPONs with offline scheduling. We focus initially on Poisson packet traffic and gated grant sizing [29,30]. For a synchronized reporting strategy, where all ONUs report their bandwidth requirements at the end of a polling cycle, we develop an analytical framework characterizing the maximum traffic load that still permits stable operation and the mean packet delay. From comparisons between our theoretical results and simulation results, we find that

- for *symmetric traffic loading*, which we define to occur when (i) the number of ONUs is an integer multiple of the number of upstream wavelength channels and (ii) the ONUs are equally loaded, the analysis correctly predicts the stability limit and approximates the delay for both synchronized reporting and immediate reporting, where the reports are immediately attached to the upstream transmission;
- for small numbers of ONUs relative to the number of upstream channels (e.g., up to five ONUs on two channels) in conjunction with asymmetric traffic loading (which occurs when the conditions for symmetric traffic are not met), the analysis correctly characterizes synchronized reporting, whereas immediate reporting gives rise to multi-cycle transmission patterns that may result in a

higher or lower stability limit compared with synchronized reporting;

- for large numbers of ONUs relative to the number of upstream transmission channels (e.g., ten or more ONUs per channel) in conjunction with only mild asymmetries in the traffic loading, the analysis approximates the stability limit and delay very well.

These analyses quantify the relationship between packet delay and network utilization. We further compare the results for Poisson packet traffic with simulations for self-similar packet traffic. We find that for the considered scenarios, self-similar traffic substantially increases delay at low to moderate loads, but also slightly increases the stability limit compared with Poisson traffic.

This paper is structured as follows. In the following subsection, we review related work. In Section II, we introduce our network model and describe the considered WDM EPON reporting, grant sizing, and grant scheduling. In Section III, we develop our analytical framework for the stability limit and packet delay characterization for Poisson packet traffic in conjunction with gated grant sizing. In Section IV, we present numerical results obtained from our analysis for symmetric traffic loads and compare them with simulation results both for Poisson and self-similar traffic. In Section V, we consider asymmetric traffic, whereby we first analyze an illustrative multicycle scenario for immediate reporting and then present numerical and simulation results, both for small and large numbers of ONUs. We summarize our conclusions in Section VI.

A. Related Work

Generally, EPON research has to date mainly relied on simulations, which have provided useful insights. However, complementing the simulations with formal mathematical analysis may lead to a deeper, fundamental understanding. Only a few existing studies have attempted to formally analyze the various aspects of EPONs. In particular, Bhatia and Bartos [31] have analyzed the collision probability for the registration messages sent by the ONUs to the OLT and dimensioned the contention window sizes for an efficient registration process. Holmberg [32] and Lannoo *et al.* [33] have analyzed EPONs with a static bandwidth allocation to the ONUs and shown that the static bandwidth allocation can meet delay constraints only at the expense of low network utilization. Bhatia *et al.* [34], Bai *et al.* [35], Lannoo *et al.* [33], Aurzada *et al.* [36], and Ngo *et al.* [37] have pursued a packet delay analysis in single-channel EPONs with dynamic bandwidth allocation.

Specific aspects of single-channel EPONs with dynamic bandwidth allocation are furthermore considered by Luo and Ansari [38,39], who have proposed and analyzed a dynamic bandwidth allocation scheme with traffic prediction assuming a Gaussian prediction error distribution. Zhu and Ma [40] have proposed a grant estimation scheme and analyzed its delay savings. Tanaka *et al.* [41] have conducted a measurement study with a real physical single-channel EPON, while Hajduczenia *et al.* [42] have compared the overhead of different passive optical network standards through simulations.

In contrast to the works reviewed so far, we analyze WDM EPONs with multiple upstream wavelength channels in this paper. The call-level performance of a WDM PON employing optical code division multiple access was analyzed in [43]. To the best of our knowledge, a packet-level analysis of WDM EPONs has so far only been attempted by Chang ([44], Section 2.4) who analyzed an offline WDM EPON with the help of a two-stage queue. The first queue models quality-of-service (QoS) distinction at the ONU and the second queue models the access of the ONU to the WDM channels. Only the second queue is of interest when comparing with the present analysis. The second queue appears to be analyzed only in terms of the average polling cycle length. However, to obtain good delay approximations, it is necessary to incorporate second moments of the involved quantities, as we do below. The model in Section 2.4 of [44] is furthermore distinct from ours in that we allow a true gated service discipline [30], rather than putting a small limit on the maximum transmission window of each ONU, which practically leads to a service discipline comparable with fixed service.

Building directly on the extensive literature on polling systems (see, e.g., [27,28]), Park *et al.* [45] derive a closed-form delay expression for a single-channel EPON model with random independent switchover times. The EPON model with independent switchover times holds only when successive upstream transmissions are separated by a random time interval sufficiently large to decorrelate successive transmissions, which would significantly reduce bandwidth utilization in practice. The literature on polling systems with correlations is relatively sparse (see, for instance, [46–51]) and considers correlations that are different from the dependencies arising in EPONs.

II. NETWORK MODEL

In this section we introduce our considered network architecture and describe the considered EPON proto-

col mechanisms for reporting, grant sizing, and grant scheduling.

A. Network Architecture

Let N be a constant denoting the number of ONUs and M be a constant denoting the number of upstream wavelength channels, whereby $N > M$; otherwise a delay analysis for single-channel EPONs with a single ONU applies [33,34,36]. Throughout, we consider ONU architectures capable of transmitting on any of the upstream wavelengths, i.e., there are no restrictions when assigning upstream transmissions to wavelengths. However, we suppose that an ONU can transmit only on one channel at a given time. Our analysis thus accommodates low-cost colorless (i.e., wavelength-independent) ONUs [52] that can be implemented with a bandpass filter in conjunction with a reflective semiconductor optical amplifier (RSOA) [53,54]. The RSOA performs remote modulation, amplification, and reflection of an optical seed signal from the OLT [55,56]. For relatively small tuning ranges, the bandpass filter can be implemented with electro-optical filters with negligible tuning times of a few nanoseconds. Larger tuning times could be masked by the transmissions of the preceding ONUs in the schedule for each wavelength. The OLT is able to simultaneously receive upstream transmissions on all M upstream wavelength channels.

Different transmission wavelengths in downstream and upstream directions result in slightly different propagation delays for the downstream and upstream directions. We introduce τ_d and τ_u (in seconds) to denote the downstream and upstream propagation delay, respectively. We remark that all analysis [except expression (14) and the delay evaluation in Subsection C of Appendix B] requires only the round-trip propagation delay $\tau_d + \tau_u$. For ease of notation, we define $2\tau := \tau_d + \tau_u$ and use this simplified notation whenever only the round-trip propagation delay is required.

The impact of the various types of overhead of different types of passive optical networks, including EPONs, was thoroughly investigated in [42,57]. We consequently neglect initially all overheads in our analysis in order not to obscure the analytical techniques to capture the fundamental system dynamics due to the polling timing structure. In Appendix A we outline how the analysis can be extended to accommodate overheads.

Let λ_i , $i = 1, \dots, N$, denote the Poissonian traffic generation rate (in packets/s) of ONU i . Let \bar{L} and σ_L denote the mean and standard deviation of the packet size (in bits). Let C denote the transmission rate (in bits/s) of an upstream transmission channel. We define the normalized traffic intensities (loads) as

$$\rho_i := \frac{\lambda_i \bar{L}}{C} \quad (1)$$

and note that $\lambda_i \bar{L}$ is the average bit rate of the traffic generated at ONU i . We define the total normalized traffic load as

$$\rho_T := \sum_{i=1}^N \rho_i. \quad (2)$$

Clearly, a necessary condition for stability is that the total normalized traffic load is less than the number of upstream wavelength channels, i.e., that

$$\rho_T < M. \quad (3)$$

B. Offline Scheduling Framework With Gated Grant Sizing and Largest Process Time Grant Scheduling

We focus in this study on a WDM EPON with offline operation, also referred to as the offline scheduling framework [20] or interleaved polling with stop [11,23]. In the offline scheduling framework with *immediate reporting*, each ONU i , $i=1, \dots, N$, appends its report of the currently queued amount of upstream traffic to the current upstream transmission. Specifically, let R_i^{n-1} denote the duration (in seconds) of the upstream transmission window requested (reported) by ONU i in cycle $n-1$; note that the duration of the requested upstream transmission window is equal to the amount of queued traffic divided by the upstream transmission bit rate. The OLT collects the reports from all ONUs before making grant sizing and grant scheduling decisions. We consider *gated* grant sizing, which sets the size of the grant for cycle n equal to the request received during the preceding cycle. Formally, let G_i^n be a random variable denoting the grant duration (in seconds) of ONU i in cycle n . For gated grant sizing, $G_i^n = R_i^{n-1}$ [29,30]. With a grant duration (length of the granted upstream transmission window) of G_i^n , ONU i can send CG_i^n bits upstream in cycle n . These CG_i^n bits of upstream traffic were generated and reported during the preceding cycle $n-1$. We briefly note that the described reporting and scheduling approach applies to EPONs. ITU-T G984 gigabit PONs (GPONs) have a fundamentally different timing structure due to their fixed frame length with each upstream frame providing an opportunity to report bandwidth demands to the OLT [also called the optical network terminal (ONT)] and each downstream frame providing the opportunity to assign grants to the ONUs. GPONs are therefore outside the scope of this study. For an elaboration of these fundamental differences and a preliminary comparative analysis of EPONs and GPONs we refer to [58].

Next, we turn to the scheduling of the grants (upstream transmission windows) G_i^n , $i=1, \dots, N$, on the M upstream wavelength channels. In general, the problem of scheduling jobs without assignment restrictions to machines so as to minimize the total length of the schedule, i.e., the so-called makespan, is NP hard. However, largest processing time first (LPT), which orders the jobs from largest to smallest and one by one schedules them on the next available machine, gives good performance [59]. The LPT competitive ratio, defined as the worst-case upper bound on the makespan compared with optimal scheduling, for scheduling on M machines is $[4/3 - 1/(3M)]$ [59]. This means that for $M=1$ machine, LPT achieves the optimal (shortest possible) schedule makespan, whereas for $M=2$ machines the LPT makespan is at most 7/6 times the optimal makespan. In the context of EPONs, the upstream wavelengths represent the machines, and the upstream transmission grants of given duration represent the jobs.

To formally model the scheduling, we decompose the set of grants $\{G_1^n, \dots, G_N^n\}$ into M (disjoint) sets I_1, \dots, I_M according to the LPT policy. Note that the length of the upstream transmission schedule (in seconds) on wavelength channel m for cycle n is given by $S_m(G_1^n, \dots, G_N^n) = \sum_{i \in I_m} G_i^n$. The maximum over all channels m , $m=1, \dots, M$, gives the total length (makespan) of the schedule as

$$S_{\max}(G_1^n, \dots, G_N^n) := \max_{m=1, \dots, M} S_m(G_1^n, \dots, G_N^n). \quad (4)$$

C. Synchronized Reporting

Toward developing an analytical framework for offline EPON analysis, we introduce the following modification to the reporting of the queued upstream traffic. The ONUs sending upstream data in a given cycle in their granted upstream transmission windows do not append a report of their current queue occupancies at the end of their upstream transmissions. Instead, only the ONU whose upstream transmission last reaches the OLT in the cycle, appends its report to the upstream transmission. The report transmissions of the other ONUs are timed such that they arrive right after the report of the last ONU, separated by guard times. With this modification, the OLT receives *synchronized* reports that reflect the queue occupancies at *all* ONUs from about the upstream propagation delay ago. Note that this reporting strategy slightly increases the cycle length due to the additional guard times. With t_g (in seconds) denoting the guard time (typical value is $t_g = 5 \mu\text{s}$), this added time is approximately $t_g[N/M]$; see Appendix A.

D. Limited Grant Sizing

Although the main focus of this study is on gated grant sizing where the grant size is set equal to the request $G_i^n = R_i^{n-1}$ [29,30], we briefly consider limited grant sizing in this section. With limited grant sizing the grant size is set equal to the request up to a prescribed maximum G_i^{\max} , i.e., $G_i^n = \min\{R_i^{n-1}, G_i^{\max}\}$ [29,30]. For limited grant sizing with maximum grant sizes proportional to the ONU loads, i.e., $G_i^{\max} = K\rho_i$ for $i=1, \dots, N$ for some constant K , the stability limit is

$$\rho_T < \frac{\sum_{i=1}^N G_i^{\max}}{2\tau + S_{\max}(G_1^{\max}, \dots, G_N^{\max})}. \quad (5)$$

To see this note that, as the load approaches the stability limit, the grant sizes of all ONUs approach their respective prescribed maximum G_i^{\max} and the cycle duration approaches its maximum duration of $2\tau + S_{\max}(G_1^{\max}, \dots, G_N^{\max})$. During this maximum length cycle, grants with total duration $\sum_{i=1}^N G_i^{\max}$ are served. We note that this stability limit holds for arbitrary packet traffic patterns, including self-similar packet traffic. We further note that the stability limit when the maximum grant sizes are not proportional to the ONU loads as well as the packet delay of limited grant sizing are to the best of our knowledge mathematically intractable.

III. DELAY AND STABILITY ANALYSIS FRAMEWORK

We consider the EPON with gated grant sizing in steady state. Recall that the grants G_i^n , $i=1, \dots, N$, allow the ONUs to send CG_i^n , $i=1, \dots, N$, bits upstream in cycle n . These CG_i^n bits of upstream traffic were generated during the preceding cycle $n-1$. The length of this preceding cycle in turn was governed by the grant durations G_i^{n-1} , $i=1, \dots, N$, in the preceding cycle, as well as the round-trip propagation delay 2τ . More specifically, the length of the preceding cycle was $2\tau + S_{\max}(G_1^{n-1}, \dots, G_N^{n-1})$. Throughout this preceding cycle, packets of mean size \bar{L} (bits) were generated at rate λ (packets/s). With synchronized reporting, these generated packets were reported at the end of cycle $n-1$ and are now served in cycle n with transmission rate C . Hence, given G_i^{n-1} , $i=1, \dots, N$, the mean of G_i^n is

$$\mathbb{E}G_i^n = \frac{[2\tau + \mathbb{E}S_{\max}(G_1^{n-1}, \dots, G_N^{n-1})]\lambda_i \bar{L}}{C}. \quad (6)$$

We note that, given $G_1^{n-1}, \dots, G_N^{n-1}$, the G_i^n concentrate strongly around their mean, since they are a mixture of Poisson variables. Therefore, we can approximate as follows:

$$\begin{aligned} \mathbb{E}S_{\max}(G_1^n, \dots, G_N^n) \\ = \mathbb{E}\mathbb{E}[S_{\max}(G_1^n, \dots, G_N^n) | G_1^{n-1}, \dots, G_N^{n-1}] \end{aligned} \quad (7)$$

$$\approx S_{\max}(\mathbb{E}G_1^n, \dots, \mathbb{E}G_N^n) \quad (8)$$

$$= S_{\max}\left(\left\{ [2\tau + \mathbb{E}S_{\max}(G_1^{n-1}, \dots, G_N^{n-1})] \frac{\lambda_i \bar{L}}{C} \right\}_{i=1, \dots, N}\right) \quad (9)$$

$$= [2\tau + \mathbb{E}S_{\max}(G_1^{n-1}, \dots, G_N^{n-1})] S_{\max}(\rho_1, \dots, \rho_N). \quad (10)$$

We define the *maximum normalized channel load* as

$$\rho^* := S_{\max}(\rho_1, \dots, \rho_N), \quad (11)$$

whereby the functional $S_{\max}(\cdot)$ is defined according to Eq. (4), and note that ρ^* can be calculated from the ρ_i , $i=1, \dots, N$.

Noting that in steady state $\mathbb{E}S_{\max}(G_1^n, \dots, G_N^n) = \mathbb{E}S_{\max}(G_1^{n-1}, \dots, G_N^{n-1})$, we obtain

$$\mathbb{E}S_{\max}(G_1^n, \dots, G_N^n) \approx \frac{2\tau\rho^*}{(1-\rho^*)}. \quad (12)$$

Hence, the system is stable if

$$\rho^* < 1. \quad (13)$$

Similar arguments for the second moment and the calculations in [36] show that the mean packet delay is approximately:

$$\mathbb{E}D(\rho^*) = 2\tau \frac{3-\rho^*}{2(1-\rho^*)} + \frac{\rho^*}{2C(1-\rho^*)} \left(\frac{\sigma_L^2}{\bar{L}} + \bar{L} \right) + \tau_u + \frac{\bar{L}}{C}. \quad (14)$$

The approximation is exact for synchronized reporting for $M=1$ and $N \geq 1$. To see this, note that the synchronized-reporting EPON with $M=1$, $N \geq 1$ is equivalent to an immediate-reporting EPON with $M=1$, $N=1$ in which the load of the one ONU is equal to the sum of the loads of the N ONUs in the synchronized-reporting EPON. In particular, when neglecting the guard times and report transmission times, all N reports are sent at essentially the same time with synchronized reporting. Equivalently, a single report can be sent in the immediate-reporting EPON. Furthermore, in the single-channel synchronized-reporting EPON the ONUs send their data one after the other on the single channel. Equivalently, the data could be sent by a single ONU. Hence, the exact mean packet delay analysis for a single-channel, single-ONU, immediate-reporting EPON from [36] gives an exact mean packet delay

analysis for the single-channel, multiple-ONU, synchronized-reporting EPON.

In addition to the delay approximation obtained by inserting ρ^* in Eq. (14), we note that the following modification of Eq. (14) gives a lower bound of the delay. The delay would be lower if it were possible to distribute the grants perfectly equally over the M channels, such that the upstream transmission window is $1/M \sum_{i=1}^N G_i^n$ on each channel. In this model, we need to replace ρ^* by the smaller *average normalized channel load* ρ_T/M . Using this quantity and the above arguments based on [36], we obtain the lower bound by inserting ρ_T/M in Eq. (14), i.e., by evaluating $ED(\rho_T/M)$. Again, this bound returns the exact mean packet delay for $M=1$, since then $\rho^* = \rho_T = \sum_{i=1}^N \rho_i$.

We furthermore define *equal channel loading* to occur when

$$S_1(\rho_1, \dots, \rho_N) = S_2(\rho_1, \dots, \rho_N) = \dots = S_M(\rho_1, \dots, \rho_N). \quad (15)$$

Note that for equal channel loading, $\rho^* = \rho_T/M$, which reduces the stability condition (13) to the necessary condition (3).

We conclude this section on the analytical framework by noting that the reasoning leading to Eq. (6) considered synchronized reporting, resulting in a relatively good analytical characterization of synchronized reporting, as demonstrated with numerical and simulation results in Section IV and Subsection V.C. We also demonstrate in Section IV that the analysis characterizes immediate reporting quite accurately for symmetric traffic loading. For asymmetric traffic loading, we show in Section V how immediate reporting gives rise to multicycle transmission patterns that lead to different stability limits than for synchronized reporting.

IV. NUMERICAL AND SIMULATION RESULTS FOR SYMMETRIC TRAFFIC

In this section, we consider the *symmetric traffic loading* cases where the number of ONUs N is an integer multiple of the number of upstream wavelengths M , i.e., $N = kM$ for some integer k , and all ONUs contribute equally to the total traffic load, i.e., $\rho_1 = \dots = \rho_N$. For these cases, $\rho^* = k\rho_1 = \rho_T/M$; inserting this load value in Eq. (14) gives the approximate mean packet delay.

A. Simulation Setup

We verify the accuracy of the analysis by comparing it with simulation results. We consider an EPON with upstream transmission bit rate $C=1$ Gbps operated with offline scheduling. We initially consider a dis-

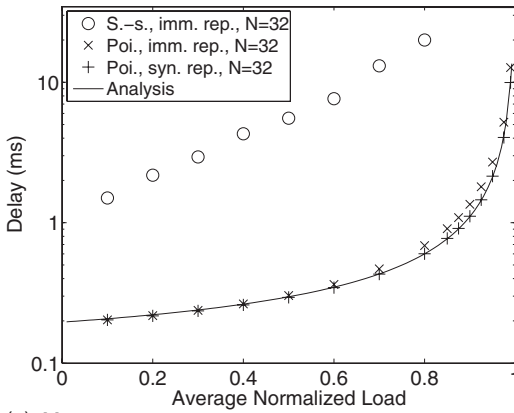
tance of 9.6 km between the OLT and ONUs, corresponding to one-way propagation delays of approximately $\tau_d = \tau_u = 9.6 \text{ km}/(200,000 \text{ km/s}) = 48 \mu\text{s}$. Each ONU i , $i=1, \dots, M$, has an independent Poisson packet generation process with rate λ_i (packets/s) and an infinite buffer for generated packets. Recent studies, e.g., [60,61], have examined packet size distributions and their impact on EPON access network delay has been investigated in [36] and found to be relatively minor. Therefore, we consider for simplicity a fixed packet size of $\bar{L}=1500$ bytes ($\sigma_L=0$) in the simulations. For Poisson traffic, the 90% confidence intervals, obtained with the method of batch means, are smaller than the point marks in the plots.

For the self-similar packet traffic simulations, each ONU independently generates self-similar packet traffic by aggregating several Pareto-distributed on-off sources [62,63]. The degree of self-similarity is characterized by the Hurst parameter H , $0.5 \leq H \leq 1$, whereby Poisson traffic has $H=0.5$, and a higher H indicates a higher degree of self-similarity. We consider a mild degree of self-similarity ($H=0.55$) and a moderately strong degree of self-similarity ($H=0.75$, which is widely considered in EPON studies).

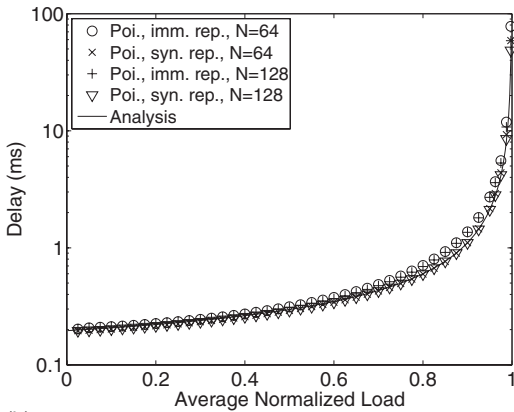
We neglect all overheads to bring out the fundamental system dynamics. We present results for the mean packet delay, defined as the delay from packet generation at an ONU until the complete reception at the OLT, as a function of the average normalized channel load ρ_T/M , whereby the total normalized load ρ_T is defined in Eq. (2).

B. Results

In Fig. 1, we present analysis results as well as simulation results for Poisson traffic for immediate and synchronized reporting for $M=1$ and 4 wavelengths. We also present simulation results for self-similar traffic with $H=0.75$ for $M=1$ for immediate reporting. We observe from Fig. 1(a) that the analytical approximation results essentially coincide with the simulation results for synchronized reporting, confirming the accuracy of the delay analysis for $M=1$ for this reporting type. From additional simulations for $N=2$, which are not plotted to avoid clutter, we observed a similarly good match for synchronized reporting. We also observe that for $N=32$, immediate reporting gives slightly higher delays than synchronized reporting (for $N=2$, the delay increase with immediate reporting was slightly smaller than for $N=32$). This is primarily because with immediate reporting only ONU i packets generated up to the end of the upstream transmission of ONU i are included in the report. Packets generated by ONU i between the end of its upstream transmission and the end of the last transmission by an ONU in the cycle are reported in



(a) $M=1$



(b) $M=4$

Fig. 1. Mean packet delay as a function of average normalized channel load ρ_T/M for an EPON with M channels and N ONUs with equal traffic load.

the next cycle. With synchronized reporting, these packets are still included in the reporting for this cycle. Thus, these packets “save” one cycle of delay.

Similar observations hold for the scenario with $M=4$ channels considered in Fig. 1(b). The analysis correctly predicts the stability limit and quite accurately characterizes the mean packet delay of these WDM EPON scenarios with symmetric traffic loads.

For self-similar traffic, which is significantly burstier than Poisson traffic, we observe substantially higher delays than for Poisson traffic. In additional simulations, we found that self-similar traffic has the same stability limit as Poisson traffic and that the mean packet delay exceeds 200 ms for a load of 0.99.

V. STABILITY LIMITS AND DELAYS FOR ASYMMETRIC TRAFFIC

In this section, we examine the cases with *asymmetric traffic loading*, e.g., when the number of (equally loaded) ONUs N is not an integer multiple of the number of upstream channels M , i.e., $N \neq kM$, or when N

$=kM$ ONUs are nonequally loaded. We first analyze the illustrative case $N=3, M=2$ (with equal ONU Poisson traffic loads) and present a summary of stability results for a range of scenarios with $N \neq kM$ equally loaded ONUs in Subsection V.B. We then present numerical and simulation results for asymmetric traffic in Subsection V.C, both for scenarios where the number of ONUs N is small relative to the number of channels M and for scenarios with $N \gg M$.

A. Case Study for $N=3, M=2$: Stability Analysis

Consider an EPON with $N=3$ ONUs and $M=2$ upstream channels and equal ONU traffic loads $\rho_1=\rho_2=\rho_3$. From the analysis in Section III, one would expect that $\rho_1 < 0.5$ is the stability condition for this system. While this is the correct stability limit for synchronized reporting, as demonstrated in Subsection V.C, for immediate reporting, a multicycle transmission pattern with unequal transmission grants arises, as illustrated in Fig. 2. This multicycle transmission pattern raises the stability limit to $\rho_1 < \sqrt{3}/3 = 1/\sqrt{3}$. Let g_1, g_2 , and g_3 denote the three steady-state expected values of the grant durations of the transmission pattern sorted in decreasing order. (In this section, we analyze the transmission patterns in terms of their long-run expected values in order to examine their impact on the capacity; a more detailed analysis incorporating second moments is conducted in Appendix B in order to examine the packet delay.) In cycle $n-2$, ONU 1 has the large upstream transmission grant of expected duration g_1 , while ONU 3 has the small grant of duration g_3 . In cycle $n-1$, these roles are reversed with ONU 3 receiving the large grant of duration g_1 and ONU 1 receiving the small grant of duration g_3 . ONU 2 receives the medium duration grant of expected duration g_2 throughout. This two-cycle pattern then repeats over a large time span, before random fluctuations eventually lead to a reversal of roles within the same pattern. For instance, ONUs 2 and 1 may exchange roles such that ONUs 2 and 3 alternate in having the large and small grant while ONU 1 always has the medium duration grant.

We analyze the stability of this two-cycle pattern by noting that the cycles $n-2$ and $n-1$ determine how much data is to be sent in cycle n . Specifically, the

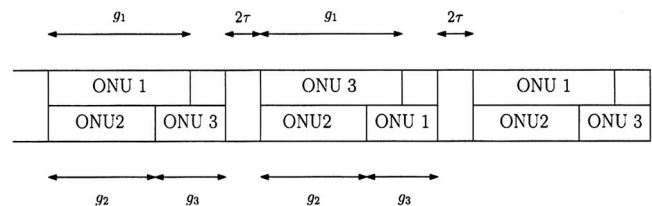


Fig. 2. Transmission pattern for $N=3, M=2$ over cycles $n-2, n-1$, and n : ONUs 1 and 3 take turns transmitting larger (smaller) upstream transmissions resulting in a stability limit of $\rho_1 < 1/\sqrt{3}$.

time between the report of ONU 1 in cycle $n-2$ and the report of ONU 1 in cycle $n-1$ is $g_2+g_3-g_1+2\tau+g_2+g_3$; whereby $g_2+g_3-g_1$ accounts for the remaining vacant period on channel 1 in cycle $n-2$, 2τ is the vacant period on both channels, and g_2+g_3 accounts for the time until the ONU 1 report is sent out in cycle $n-1$. Thus, on average (near the stability limit), ONU 1 accumulates $\lambda_1\bar{L}(g_2+g_3-g_1+2\tau+g_2+g_3)$ bits of upstream traffic between sending its report in cycle $n-2$ and sending its report in cycle $n-1$. Equivalently, ONU 1 accumulates on average a traffic amount that requires a grant duration of $\rho_1(g_2+g_3-g_1+2\tau+g_2+g_3)$ to be requested (reported) in cycle $n-1$ and then used for upstream transmission in cycle n . Analyzing ONUs 2 and 3 analogously, we obtain for the upstream grant durations of ONUs 1, 2, and 3, respectively, in cycle n :

$$g_1 = \rho_1(g_2 + g_3 - g_1 + 2\tau + g_2 + g_3), \quad (16)$$

$$g_2 = \rho_1(g_3 + 2\tau + g_2), \quad (17)$$

$$g_3 = \rho_1(2\tau + g_1). \quad (18)$$

For $\rho_1 < \sqrt{3}/3$ this system of equations has the solution

$$\begin{aligned} g_1 &= \frac{2\tau\rho_1(1+3\rho_1)}{1-3\rho_1^2}, & g_2 &= \frac{2\tau\rho_1(1+2\rho_1)}{1-3\rho_1^2}, \\ g_3 &= \frac{2\tau\rho_1(1+\rho_1)}{1-3\rho_1^2}. \end{aligned} \quad (19)$$

Intuitively, the multicycle upstream transmission patterns are due to the unequal lengths of the periods between successive reports (bandwidth requests) with immediate reporting. With synchronized reporting, the reports from all ONUs cover the same time period, namely, the full length of a cycle. Hence, multicycle upstream transmission patterns do not arise with synchronized reporting.

B. Stability Limits for Immediate Reporting for Selected Scenarios With $N \neq kM$ and Equal ONU Loads

In this section we report stability limits for a range of scenarios where the number of equally loaded ONUs N is not an integer multiple of the number of upstream channels M . We obtained these stability results by applying the analytical strategy presented for the case study in Subsection V.A analogously to the individual scenarios. Formally, we represent the multicycle upstream transmission patterns as permutations of N points (ONUs). Suppose that the stability limit is attained for an upstream transmission pattern with a period of d , $d \geq 1$, cycles. Denote

$$\pi^j = \begin{pmatrix} 1 & 2 & \cdots & N \\ \pi^j(1) & \pi^j(2) & \cdots & \pi^j(N) \end{pmatrix}, \quad j = 1, \dots, d, \quad (20)$$

for permutations of N points with the interpretation that $\pi^j(i) = i'$ means that ONU i has the i' 'th longest upstream transmission grant in the j 'th step of the pattern. For instance, the two-cycle pattern in the case study in Subsection V.A is represented by

$$\pi^1 = \begin{pmatrix} 1 & 2 & 3 \\ 1 & 2 & 3 \end{pmatrix}, \quad \pi^2 = \begin{pmatrix} 1 & 2 & 3 \\ 3 & 2 & 1 \end{pmatrix}. \quad (21)$$

We observe from Table I that, for the considered scenarios, immediate reporting results in higher stability limits than synchronized reporting, which is not always the case as demonstrated in Subsection V.C. We also observe from Table I that for the considered scenarios with $N/M = 3/2$ with equal ONU load, the stability limit is $\rho_1 < 1/\sqrt{3}$. A general proof of such stability limits for immediate reporting is an interesting direction for future research.

C. Numerical and Simulation Results

Figure 3(a) gives analytical and simulation delay results for Poisson traffic for $M=2$ channels and $N=3$ ONUs, both for equal (uniform) ONU loads, i.e., $\rho_1 = \rho_2 = \rho_3$, and nonequal (weighted) ONU loads with $\rho_1 = 2\rho_2 = 2\rho_3$ [which constitute equal channel loading, cf. Eq. (15)]. We present analytical results obtained with the analytical framework of Section III, which considers synchronized reporting, and with the delay analysis for immediate reporting for the case $N=3$, $M=2$ with equal ONU loads given in Appendix B. We observe from Fig. 3(a) that the simulation results for synchronized reporting confirm the stability limit given by Eq. (13), which for the considered equal ONU load scenario is $\rho^* = 2\rho_1 < 1$, i.e., $\rho_T < 3/2$, and for the considered weighted load scenario is $\rho^* = \rho_1 < 1$, i.e., $\rho_T < 2$. For immediate reporting, the results in Fig. 3 confirm the stability limit $\rho_1 < 1/\sqrt{3}$, i.e., $\rho_T < \sqrt{3} \approx 1.732$ for equal ONU loads. For the considered weighted scenario, we observe from Fig. 3 a stability limit of $\rho_T < 2$ for immediate reporting, which we have confirmed by analysis analogous to Subsection V.A. In fact for the considered weighted scenario, immediate reporting does not lead to a multicycle transmission pattern.

Regarding the mean packet delay, we observe from Fig. 3(a) that for these scenarios with N of the same order of magnitude as M , the approximation obtained with ρ^* in Eq. (14) is rather coarse. On the other hand, the detailed delay analysis of Appendix B correctly characterizes the delay for immediate reporting. We further note that the lower bound obtained by inserting $\rho_T/M = 3\rho_1/2$ in Eq. (14) corresponds to the delay approximation curve for the considered weighted load

TABLE I

STABILITY LIMITS AND CORRESPONDING TRANSMISSION PATTERNS FOR POISSON TRAFFIC FOR SELECTED COMBINATIONS OF NUMBER OF CHANNELS M AND NUMBER OF ONUS N WITH EQUAL ONU LOADS^a

M	N	syn. rep. $\rho_1 <$	imm. rep. $\rho_1 <$	π^2
2	3	1/2	$1/\sqrt{3}$	$\begin{pmatrix} 1 & 2 & 3 \\ 3 & 2 & 1 \end{pmatrix}$
2	5	1/3	$\frac{1}{18}[(361-18\sqrt{354})^{1/3} + (361+18\sqrt{354})^{1/3}-5]=0.371872$	$\begin{pmatrix} 1 & 2 & 3 & 4 & 5 \\ 5 & 4 & 3 & 2 & 1 \end{pmatrix}$
2	7	1/4	0.27573	$\begin{pmatrix} 1 & 2 & 3 & 4 & 5 & 6 & 7 \\ 7 & 6 & 5 & 4 & 3 & 2 & 1 \end{pmatrix}$
3	4	1/2	$1/\sqrt{3}$	$\begin{pmatrix} 1 & 2 & 3 & 4 \\ 4 & 2 & 3 & 1 \end{pmatrix}$
4	5	1/2	$1/\sqrt{3}$	$\begin{pmatrix} 1 & 2 & 3 & 4 & 5 \\ 5 & 2 & 3 & 4 & 1 \end{pmatrix}$
4	6	1/2	$1/\sqrt{3}$	$\begin{pmatrix} 1 & 2 & 3 & 4 & 5 & 6 \\ 6 & 5 & 3 & 4 & 2 & 1 \end{pmatrix}$
10	15	1/2	$1/\sqrt{3}$	$\begin{pmatrix} 1 & 2 & 3 & 4 & 5 & 6 & 7 & 8 & 9 & 10 & 11 & 12 & 13 & 14 & 15 \\ 11 & 12 & 13 & 14 & 15 & 6 & 7 & 8 & 9 & 10 & 1 & 2 & 3 & 4 & 5 \end{pmatrix}$

^aAll patterns have a period of $d=2$ and $\pi^1 = \begin{pmatrix} 1 & 2 \dots N \\ 1 & 2 \dots N \end{pmatrix}$. The stability limits with synchronized reporting as obtained from Eq. (13) are given for reference.

case plotted in Fig. 3(a), which indeed provides a lower bound for the delays with equal ONU load.

In Fig. 3(b) we plot simulation delay results for self-similar traffic; we also include the analysis curves for the equal ONU load scenario (U) from Fig. 3(a) for reference. The top two curves in Fig. 3(b) are for limited grant sizing; all others are for gated grant sizing. We consider limited grant sizing with $G^{\max}=15,000$ byte for the equal ONU load scenario (U) and maximum grant sizes $G_1^{\max}=2G_2^{\max}=2G_3^{\max}=30,000$ byte for the nonequal ONU load (W) scenario. We observe that the stability condition (5) accurately characterizes the stability limit of $\rho_T < 1.071$ (corresponding to an average normalized load of 0.54) for the U scenario and $\rho_T < 1.429$ (average normalized load of 0.71) for the W scenario.

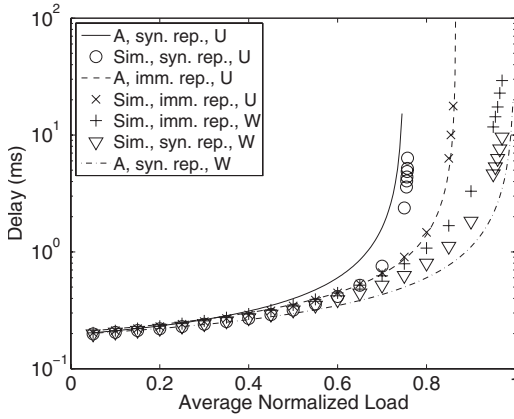
We next turn to the results for gated grant sizing, which are all for the U scenario. We observe for synchronized reporting that both the self-similar traffic with $H=0.55$ and $H=0.75$ achieve a higher stability limit than the Poisson traffic. From inspection of the grant sizes in the simulations, we found that the higher stability limit with self-similar traffic is due to fluctuations of the grant sizes among the three ONUs that persist even at high loads and correspondingly long grants. In contrast, for Poisson packet traffic, the grant sizes of all three ONUs become nearly equal when the grants become long. The equal grant sizes of the three ONUs are a worst case in the sense that they limit the total load to $\rho_T < 3/2$ (i.e., the average

normalized load to 0.75). The unequal grant sizes with self-similar traffic allow for better utilization of the two channels with LPT scheduling and hence a higher stability limit.

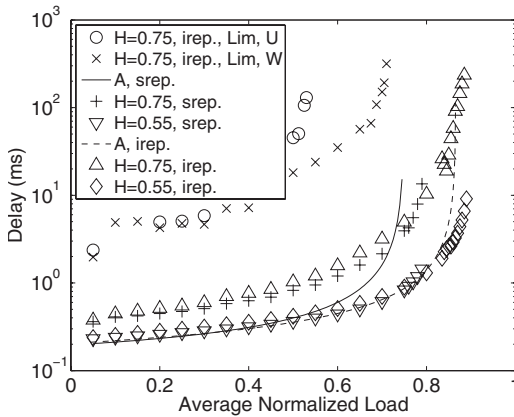
Similarly, for immediate reporting, we observe a higher stability limit for self-similar traffic than for Poisson traffic. From detailed grant size traces we found that self-similar traffic gives rise to the same pattern as depicted for Poisson traffic in Fig. 2. However, the grant sizes remain quite variable even as they grow large. This variability often leads to very large grants g_1 and rather small g_3 , reducing the idle period on the top channel in Fig. 2.

Overall, we find from these results for gated grant sizing for self-similar traffic that the corresponding analysis for Poisson traffic provides a useful reference: At low to moderate loads, self-similar traffic has higher mean delays than indicated by the Poisson analysis, especially when the degree of self-similarity is relatively high. As the load grows large, the delay of self-similar traffic reaches the vicinity of the corresponding delays from the Poisson analysis, and eventually, self-similar traffic reaches higher stability limits than Poisson traffic.

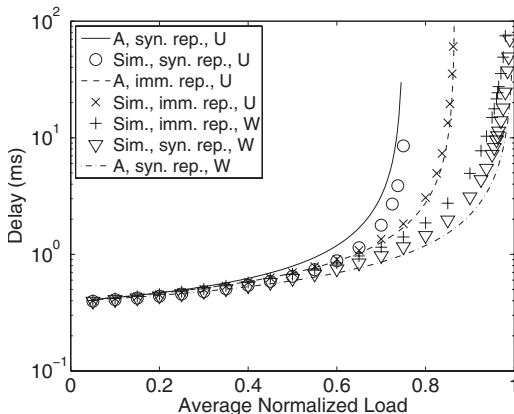
In Fig. 3(c), we evaluate the same settings as in Fig. 3(a) for a doubled OLT-ONU distance of 19.2 km. We observe that the increased propagation delay results in an upward shift of all delay curves. The analysis continues to characterize the delays quite accurately.



(a) Poisson traffic, 9.6 km OLT-ONU distance



(b) Self-similar traffic, 9.6 km OLT-ONU distance



(c) Poisson traffic, 19.2 km OLT-ONU distance

Fig. 3. Mean packet delay as a function of average normalized channel load ρ_T/M for $M=2$ channels and $N=3$ ONUs for equal [uniform (U)] ONU loads with $\rho_1=\rho_2=\rho_3$ and nonequal [weighted (W)] loads with $\rho_1=2\rho_2=2\rho_3$.

Figure 4 presents delay results for $M=2$ channels and $N=4$ ONUs with loads $\rho_1=2\rho_2=2\rho_3=2\rho_4$ and $N=5$ ONUs with loads $\rho_1=\rho_2=\rho_3=2\rho_4=2\rho_5$ for both immediate and synchronized reporting (the analytical results are obtained with the framework from Section III). For the considered $N=4$ scenario, the stability

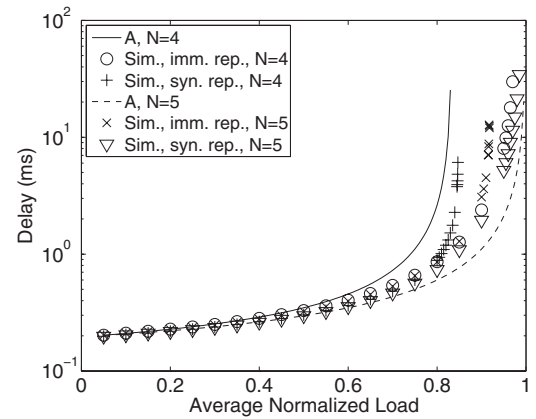


Fig. 4. Packet delay as a function of average normalized channel load ρ_T/M for $M=2$ channels and $N=4$ ONUs with loads $\rho_1=2\rho_2=2\rho_3=2\rho_4$ and $N=5$ ONUs with loads $\rho_1=\rho_2=\rho_3=2\rho_4=2\rho_5$.

condition (13) can be expressed as $\rho^*=3\rho_2 < 1$, i.e., $\rho_T < 5/3$. We observe from Fig. 4 that the simulation results for synchronized reporting confirm this stability limit. For immediate reporting, an analysis analogous to Subsection V.A gives a stability limit of $\rho_T < \frac{5}{8}(\sqrt{17}-1) \approx 1.95194$ [in conjunction with the multicycle upstream transmission pattern $\pi^2 = \begin{pmatrix} 1 & 2 & 3 & 4 \\ 4 & 3 & 2 & 1 \end{pmatrix}$], which is confirmed by the simulation results.

For the considered $N=5$ scenario, which achieves equal channel loading, the simulation results confirm the $\rho_T < M$ stability limit for synchronized reporting. With immediate reporting an analysis following Section V.A shows that the multicycle transmission pattern $\pi^2 = \begin{pmatrix} 1 & 2 & 3 & 4 & 5 \\ 3 & 2 & 1 & 5 & 4 \end{pmatrix}$ arises with the stability limit

$$\rho_T < 2 \left[\frac{(116 - 6\sqrt{78})^{1/3}}{6} + \frac{(58 + 3\sqrt{78})^{1/3}}{32^{2/3}} - \frac{2}{3} \right] \approx 1.836,$$

as confirmed by simulations. Note that for this $N=5$ scenario, immediate reporting results in a lower stability limit than synchronized reporting.

The numbers of ONUs considered in the preceding Figs. 3 and 4 were relatively small to highlight the effects possible with asymmetric loads and the transmission patterns arising with immediate reporting. We next consider in Fig. 5 a practically more relevant scenario with $M=4$ channels and a moderately large number of $N=60$ ONUs with unequal loads. We observe from this figure that for this typical scenario with $N \gg M$, which achieves equal channel loading, immediate and synchronized reporting give rather similar delay performance. The analytical framework from Section III correctly predicts the stability limit and provides an accurate delay approximation.

We next consider a scenario with a slightly smaller number of ONUs and unequal channel loading in Fig. 6. We observe from Fig. 6 that for synchronized reporting, the stability condition $\rho^*=16\rho=16\rho_T/61 < 1$,

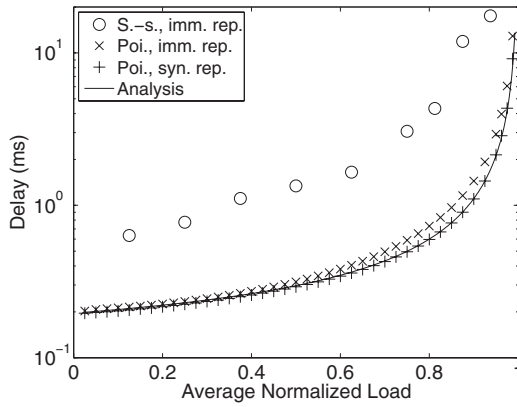


Fig. 5. Packet delay as a function of average normalized channel load ρ_T/M for $M=4$ channels and $N=60$ ONUs of which 16 have regular load ρ , 32 have half-load $\rho/2$, 8 have double-load 2ρ , and 4 have quadruple-load 4ρ .

i.e., $\rho_T < 61/16 = 3.8125$ closely matches the observed simulation results, and the delay approximation obtained by inserting ρ^* in Eq. (14) reasonably closely characterizes the actual mean packet delays. We further observe from Fig. 6 that immediate and synchronized reporting perform quite similarly, with immediate reporting achieving a slightly higher stability limit.

The results for self-similar traffic for $H=0.75$ in Figs. 5 and 6 indicate that self-similar traffic experiences higher delay. In both scenarios, self-similar traffic achieves an average normalized load approaching one.

Generally, when the ONU loads are relatively similar and the ratio of number of ONUs to number of upstream channels N/M grows large, then we approach the symmetric traffic loading case of Section IV. As we approach symmetric traffic loading, the analytical framework of Section III provides a good stability and delay characterization of synchronized reporting. Furthermore, immediate and synchronized reporting per-

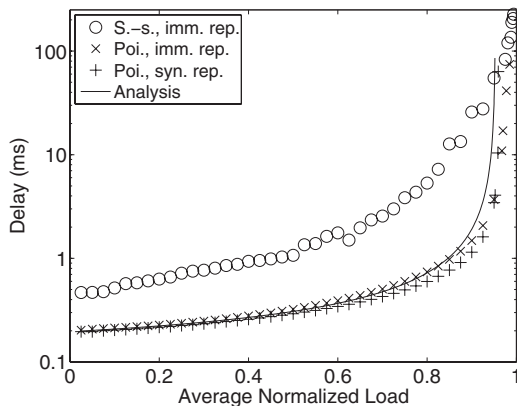


Fig. 6. Packet delay as a function of average normalized channel load ρ_T/M for $M=4$ channels and $N=41$ ONUs of which 29 have regular load ρ , 8 have double-load 2ρ , and 4 have quadruple-load 4ρ .

form very similarly as we approach symmetric traffic loading; hence, the analytical framework also characterizes immediate reporting quite accurately.

VI. CONCLUSION

In this study we have examined the stability limit and packet delay in offline WDM EPONs through probabilistic analysis and simulations. We summarize the stability limits in Table II. In particular, for synchronized reporting where all ONUs report their bandwidth requirements at the end of a cycle, the total normalized load must be less than the number of channels M when the channels are equally loaded. This equal channel loading is achieved when the decomposition of the normalized loads ρ_i , $i=1, \dots, N$, over the upstream channels results in makespans of equal length. Symmetric traffic loading, which we define to occur when the number of ONUs N is an integer k multiple of M , and all N ONUs have equal load is a special case of equal channel loading. For general asymmetric traffic loading, the longest makespan of the decomposition of the normalized loads into M sets according to the scheduling policy, i.e., the maximum normalized channel load [Eq. (11)], governs the stability limit for synchronized reporting.

For immediate reporting, where the bandwidth requests are immediately attached to the end of each upstream transmission, we discovered a more complex stability behavior. Only for symmetric traffic loading, or for traffic that is a reasonably close approximation of symmetric traffic loading, which is likely to occur typically in practice when the number of ONUs N is significantly larger than the number of upstream channels M and the normalized traffic loads of the ONUs are similar, does the EPON obey the $\rho_T < M$ stability limit. When the number of ONUs is relatively small, i.e., is on the same order as the number of channels, and the traffic loads are asymmetric (even if they

TABLE II
SUMMARY OF STABILITY AND DELAY RESULTS FOR DIFFERENT REPORTING STRATEGIES AND TRAFFIC LOAD SCENARIOS FOR POISSON TRAFFIC AND GATED GRANT SIZING^a

Reporting	Symmetric loading (i.e., $N=kM$ and equal ONU loads) or $N \gg M$	Equal channel loads	General asymmetric loading
Synchronized	$\rho^* = \rho_T/M < 1$	$\rho^* = \rho_T/M < 1$	$\rho^* < 1$
Immediate	$\rho^* = \rho_T/M < 1$	patterns	patterns

^a ρ_T is the total traffic load defined in Eq. (2) and ρ^* is the maximum normalized channel load as defined in Eq. (11). The multicycle transmission patterns with immediate reporting can result in a lower or higher stability limit than for synchronized reporting. Mean packet delay approximations are given by inserting the left-hand sides of the stability limits in Eq. (14).

still achieve equal channel loading), then multicycle upstream transmission patterns arise. These multicycle transmission patterns can be formally analyzed following the approaches demonstrated in Subsection V.A and Appendix B and can lead to either a lower or higher stability limit compared with the corresponding limit for synchronized reporting.

We found that inserting the normalized load parameters on the left-hand sides of the stability limits summarized in Table II in the delay expression (14) obtained from our analytical framework gives approximations of the mean packet delay. The approximations are quite accurate for the symmetric traffic loading and scenarios with $N \gg M$, corresponding to the leftmost column of Table II. For the synchronized reporting cases in the middle and rightmost column of Table II the approximation becomes coarse.

For limited grant sizing with the maximum grant sizes proportional to the ONU traffic loads, we provided the analytical stability limit for arbitrary packet traffic, including self-similar traffic. For gated grant sizing, we observed that the higher variabilities in self-similar packet traffic generally result in higher packet delays, but can also lead to better utilization of the upstream channels than for Poisson traffic.

More accurate delay approximations for these synchronized reporting scenarios as well as delay analyses for the immediate reporting scenarios with upstream transmission patterns are important directions for future research. Another important avenue for future research appears to examine novel grant sizing strategies that eliminate unused periods on the wavelength channels due to the different lengths $S_m(G_1^n, \dots, G_N^n)$, $m = 1, \dots, M$, of the upstream transmission schedules. Scaling the transmission grants for wavelength m by $[\min_{m=1, \dots, M} S_m(G_1^n, \dots, G_N^n)]/S_m(G_1^n, \dots, G_N^n)$ would equalize the upstream transmission schedules on the wavelengths. Yet another interesting direction for future research is to combine the packet-switched service considered in this study with a dynamically configured circuit-switched service, e.g., for very large file transfers or continuous media streaming applications, similar to the architecture examined in [64].

APPENDIX A: EXTENSION OF ANALYTICAL FRAMEWORK TO OVERHEADS

In this appendix we outline how the analytical framework of Section III can be extended to accommodate the various overheads in an EPON and discuss the impact of overheads on the stability and delay. We denote o_c (in seconds) for the overhead that occurs once per cycle, such as the schedule computing time in the OLT and the transmission time of the GATE message to the first ONU in the schedule (on each wave-

length); subsequent GATE message transmissions are masked by the transmission of the first ONU. This per-cycle overhead effectively lengthens the idle period between the arrival of the end of the last upstream transmission of a cycle at the OLT and the arrival of the beginning of the first upstream transmission of the next cycle from 2τ to $(2\tau + o_c)$. Thus, substituting $(2\tau + o_c)$ for 2τ throughout the analysis accounts for the per-cycle overhead. This per-cycle overhead does not affect the stability limit for gated grant sizing since for heavy load and correspondingly long grants, the idle period $(2\tau + o_c)$ becomes negligible. In contrast, the stability limit for limited grant sizing is reduced by the per-cycle overhead; see Eq. (5).

We denote o_g (in seconds) for the overhead associated with an upstream transmission of a given ONU, such as the transmission time of the report message and the guard time between ONU transmissions. This per-grant overhead has two main effects: (i) the grant durations of the preceding cycle G_i^{n-1} in Eq. (6) are lengthened to $G_i^{n-1} + o_g$, and (ii) the expected grant duration $\mathbb{E}G_i^n$ in Eq. (6) is extended by o_g . The first effect is intractable with the analytical framework in Section III since in the evaluation of Eq. (10) the functional $\mathbb{E}S_{\max}(\cdot)$ would involve grant durations G_i^n on the left-hand side and duration $G_i^n + o_g$ on the right-hand side. The second effect can be approximated by adding $S_{\max}(o_g, \dots, o_g) \approx o_g \lceil N/M \rceil$ to the numerator of Eq. (12). Overall, the per-grant overhead does not affect the stability limit of gated grant sizing since the fixed per-grant overhead becomes negligible as the grant durations grow large for heavy traffic.

We denote o_p (in bits) for the overhead associated with a packet transmission, such as interpacket gap and preamble. This per-packet overhead effectively lengthens the average packet length from \bar{L} to $\bar{L} + o_p$. Note that this packet lengthening increases the normalized ONU load from $\lambda_i \bar{L}/C$ to $\lambda_i (\bar{L} + o_p)/C$; thus, reducing the stability limit by a factor of $\bar{L}/(\bar{L} + o_p)$.

APPENDIX B: CASE STUDY FOR $N=3, M=2$: DELAY ANALYSIS FOR IMMEDIATE REPORTING

1. RECURRENCE EQUATIONS AND FIRST MOMENTS

Let $G_{(i)}^n$, $i = 1, 2, 3$, be random variables denoting the grant durations (in seconds) in cycle n sorted in decreasing order. We consider a Poissonian packet generation process with rate λ (packets/s) at each node and denote $\text{Poi}[\omega]$ for a random variable with Poisson distribution with parameter ω . Retracing the analysis in Subsection V.A leading to the system of equations (16)–(18) we obtain

$$G_{(1)}^n = \frac{\bar{L}}{C} \text{Poi}[\lambda(G_{(2)}^{n-2} + G_{(3)}^{n-2} - G_{(1)}^{n-2} + 2\tau + G_{(2)}^{n-1} + G_{(3)}^{n-1})], \quad (22)$$

$$G_n^{(2)} = \frac{\bar{L}}{C} \text{Poi}[\lambda(G_{(3)}^{n-2} + 2\tau + G_{(2)}^{n-1})], \quad (23)$$

$$G_n^{(3)} = \frac{\bar{L}}{C} \text{Poi}[\lambda(2\tau + G_{(1)}^{n-1})]. \quad (24)$$

Consider the system in steady state. Then, $g_i := \mathbb{E}G_{(i)}^{n-1} = \mathbb{E}G_{(i)}^n$ and $s_i := \mathbb{E}(G_{(i)}^{n-1})^2 = \mathbb{E}(G_{(i)}^n)^2$, $i=1, 2, 3$. Taking expectations gives equations (16)–(18).

2. SECOND MOMENTS

Now we take second moments of Eqs. (22)–(24). Noting that for a Poisson random variable X with parameter ω , we have $\mathbb{E}X = \omega$ and $\mathbb{E}X^2 = \omega + \omega^2$, we obtain

$$s_1 = \frac{\bar{L}}{C} g_1 + \rho^2 \mathbb{E}(G_{(2)}^{n-2} + G_{(3)}^{n-2} - G_{(1)}^{n-2} + 2\tau + G_{(2)}^{n-1} + G_{(3)}^{n-1})^2, \quad (25)$$

$$s_2 = \frac{\bar{L}}{C} g_2 + \rho^2 \mathbb{E}(G_{(3)}^{n-2} + 2\tau + G_{(2)}^{n-1})^2, \quad (26)$$

$$s_3 = \frac{\bar{L}}{C} g_3 + \rho^2 \mathbb{E}(2\tau + G_{(1)}^{n-1})^2. \quad (27)$$

We proceed to rewrite the right-hand sides such that only the known variables g_i and the unknowns s_i appear. For this purpose, we need to introduce some more notation. We use the following abbreviations:

$$g_{i,j}^0 := \mathbb{E}[G_{(i)}^n G_{(j)}^n], \quad g_{i,j}^1 := \mathbb{E}[G_{(i)}^{n-1} G_{(j)}^n].$$

Note that $s_i = g_{i,i}^0$ and $g_{i,j}^0 = g_{j,i}^0$. Thus, there are 15 unknowns.

For example, Eq. (27) can be rewritten as follows:

$$s_3 = \frac{\bar{L}}{C} g_3 + \rho^2 [(2\tau)^2 + 2 \cdot 2\tau g_1 + s_1]. \quad (28)$$

On the other hand, the crucial term in Eq. (26) is

$$\begin{aligned} & \mathbb{E}(G_{(3)}^{n-2} + 2\tau + G_{(2)}^{n-1})^2 \\ &= s_3 + 2\mathbb{E}[G_{(3)}^{n-2}(2\tau + G_{(2)}^{n-1})] + \mathbb{E}(2\tau + G_{(2)}^{n-1})^2 \\ &= s_3 + 2 \cdot 2\tau g_3 + 2\mathbb{E}[G_{(3)}^{n-2} G_{(2)}^{n-1}] + (2\tau)^2 + 2 \cdot 2\tau g_2 + s_2. \end{aligned}$$

Thus, Eq. (26) becomes

$$s_2 = \frac{\bar{L}}{C} g_2 + \rho^2 [s_3 + 2 \cdot 2\tau g_3 + 2g_{3,2}^1 + (2\tau)^2 + 2 \cdot 2\tau g_2 + s_2]. \quad (29)$$

Similarly, Eq. (25) becomes

$$\begin{aligned} s_1 &= \frac{\bar{L}}{C} g_1 + \rho^2 [g_{2,2}^0 + g_{2,3}^0 - g_{2,1}^0 + 2\tau g_2 + g_{2,2}^1 + g_{2,3}^1 + g_{3,3}^0 \\ &\quad - g_{1,3}^0 + 2\tau g_3 + g_{3,2}^1 + g_{3,3}^1 - g_{1,1}^0 - 2\tau g_1 - g_{1,2}^1 - g_{1,3}^1 \\ &\quad + (2\tau)^2 + 2\tau g_2 + 2\tau g_3 + g_{2,2}^0 + g_{2,3}^0 + g_{3,3}^0]. \quad (30) \end{aligned}$$

Now, let \mathcal{F}^n be the information given the data from the n th cycle. We can obtain relations between the cycles in the following way:

$$\begin{aligned} g_{1,1}^1 &= \mathbb{E}[G_{(1)}^{n-1} G_{(1)}^n] \\ &= \mathbb{E}[G_{(1)}^{n-1} \mathbb{E}(G_{(1)}^n | \mathcal{F}^{n-1})] \\ &= \mathbb{E}[G_{(1)}^{n-1} \rho(G_{(2)}^{n-2} + G_{(3)}^{n-2} - G_{(1)}^{n-2} + 2\tau + G_{(2)}^{n-1} + G_{(3)}^{n-1})] \\ &= \rho(g_{2,1}^1 + g_{3,1}^1 - g_{1,1}^1 + 2\tau g_1 + g_{1,2}^0 + g_{1,3}^0). \quad (31) \end{aligned}$$

The same way we get, e.g.,

$$\begin{aligned} g_{3,2}^1 &= \mathbb{E}[G_{(3)}^{n-2} G_{(2)}^{n-1}] \\ &= \mathbb{E}[G_{(3)}^{n-2} \mathbb{E}(G_{(2)}^{n-1} | \mathcal{F}^{n-2})] \\ &= \mathbb{E}[G_{(3)}^{n-2} \rho(G_{(3)}^{n-3} + 2\tau + G_{(2)}^{n-2})] \\ &= \rho \mathbb{E}(G_{(3)}^{n-2} G_{(3)}^{n-3}) + 2\tau \rho g_3 + \rho \mathbb{E}(G_{(3)}^{n-2} G_{(2)}^{n-2}) \\ &= \rho(g_{3,3}^1 + 2\tau g_3 + g_{2,3}^0). \quad (32) \end{aligned}$$

Analogously, the following relations can be derived:

$$g_{1,2}^1 = \rho(g_{3,1}^1 + 2\tau g_1 + g_{1,2}^0), \quad (33)$$

$$g_{1,3}^1 = \rho(g_1 2\tau + g_{1,1}^0), \quad (34)$$

$$g_{2,1}^1 = \rho(g_{2,2}^1 + g_{3,2}^1 - g_{1,2}^1 + 2\tau g_2 + g_{2,2}^0 + g_{2,3}^0), \quad (35)$$

$$g_{2,2}^1 = \rho(g_{3,2}^1 + 2\tau g_2 + g_{2,2}^0), \quad (36)$$

$$g_{2,3}^1 = \rho(2\tau g_2 + g_{1,2}^0), \quad (37)$$

$$g_{3,1}^1 = \rho(g_{2,3}^1 + g_{3,3}^1 - g_{1,3}^1 + 2\tau g_3 + g_{2,3}^0 + g_{3,3}^0), \quad (38)$$

$$g_{3,3}^1 = \rho(2\tau g_3 + g_{1,3}^0). \quad (39)$$

Given \mathcal{F}_{n-1} , $G_{(i)}^n$ and $G_{(j)}^n$ are independent for $i \neq j$; thus, we further obtain

$$\begin{aligned} g_{1,2}^0 &= \rho^2 [g_{2,3}^0 + 2\tau g_2 + g_{2,2}^1 + g_{3,3}^0 + 2\tau g_3 + g_{3,2}^1 - g_{1,3}^0 \\ &\quad - 2\tau g_1 - g_{1,2}^1 + 2\tau g_3 + (2\tau)^2 + 2\tau g_2 + g_{3,2}^1 + g_2 2\tau \\ &\quad + g_{2,2}^0 + g_{3,3}^1 + 2\tau g_3 + g_{2,3}^0], \quad (40) \end{aligned}$$

$$g_{1,3}^0 = \rho^2[2\tau(g_2 + g_3 - g_1 + 2\tau + g_2 + g_3) + g_{2,1}^1 + g_{3,1}^1 - g_{1,1}^1 + 2\tau g_1 + g_{2,1}^0 + g_{3,1}^0], \quad (41)$$

$$g_{2,3}^0 = \rho^2[2\tau(g_3 + 2\tau + g_2) + g_{3,1}^1 + 2\tau g_1 + g_{1,2}^0]. \quad (42)$$

Equations (28)–(42) are 15 linear equations for 15 unknowns and can thus be solved for all $g_{i,j}^k$. Doing so we obtain s_1 , s_2 , and s_3 .

3. DELAY EVALUATION

We consider case by case the delay of a packet generated by ONU i with respect to the timing of the packet generation. From the illustration in Fig. 2 we observe six different cases for the timing of the packet generation, which we index by j , $j=1, \dots, 6$, as detailed in the following listing. For a given combination of ONU i and timing case j , we denote $D_{i,j}$ for the corresponding packet delay and $p_{i,j}$ for the probability of occurrence of the combination i,j . We obtain the overall mean packet delay as

$$D = \frac{1}{3} \sum_{i=1, \dots, 3, j=1, \dots, 6} D_{i,j} p_{i,j}.$$

In the delay expressions, we denote $\mathbb{E}\text{Res}(G)$ for the mean residual lifetime of the distribution of G :

$$\mathbb{E}\text{Res}(G_{(i)}) = \frac{\mathbb{E}(G_{(i)})^2}{2\mathbb{E}G_{(i)}} = \frac{s_i}{2g_i}.$$

We also need

$$\begin{aligned} \mathbb{E}\text{Res}(G_{(2)} + G_{(3)} - G_{(1)}) &= \frac{\mathbb{E}(G_{(2)} + G_{(3)} - G_{(1)})^2}{2\mathbb{E}(G_{(2)} + G_{(3)} - G_{(1)})} \\ &= \frac{s_2 + g_{2,3}^0 - g_{2,1}^0 + s_3 - g_{3,1}^0 + s_1}{2(g_2 + g_3 - g_1)}. \end{aligned}$$

1,1 Packet is generated at ONU 1 during the 2τ time period before a cycle in which ONU 1 has the longest grant: $D_{1,1} = \tau_u + g_2 + g_3 + 2\tau + g_2 + \rho \times \mathbb{E}\text{Res}(G_{(3)}) + \tau_u + \bar{L}/C$, $p_{1,1} = 2\tau/(2\tau + g_2 + g_3 + 2\tau + g_2 + g_3)$.

1,2 Packet is generated at ONU 1 while ONU 1 is sending the longest grant: $D_{1,2} = \mathbb{E}\text{Res}(G_{(1)}) + g_2 + g_3 - g_1 + 2\tau + g_2 + \rho \times \mathbb{E}\text{Res}(G_{(3)}) + \tau_u + \bar{L}/C$, $p_{1,2} = g_1/(2\tau + g_2 + g_3 + 2\tau + g_2 + g_3)$.

1,3 Packet is generated at ONU 1 during a cycle in which ONU 1 has the longest grant, but ONU 1 has finished sending: $D_{1,3} = \mathbb{E}\text{Res}(G_{(2)} + G_{(3)} - G_{(1)}) + 2\tau + g_2 + g_3 + 2\tau + \rho \times \mathbb{E}\text{Res}(G_{(1)}) + \tau_u + \bar{L}/C$, $p_{1,3} = (g_2 + g_3 - g_1)/(2\tau + g_2 + g_3 + 2\tau + g_2 + g_3)$.

1,4 Packet is generated at ONU 1 during a 2τ period

before ONU 1 has the shortest grant: $D_{1,4} = \tau_u + g_2 + g_3 + 2\tau + \rho \times \mathbb{E}\text{Res}(G_{(1)}) + \tau_u + \bar{L}/C$, $p_{1,4} = 2\tau/(2\tau + g_2 + g_3 + 2\tau + g_2 + g_3)$.

1,5 Packet is generated at ONU 1 during a cycle when ONU 1 has the shortest grant and ONU 2 is sending: $D_{1,5} = \mathbb{E}\text{Res}(G_{(2)}) + g_3 + 2\tau + \rho \times \mathbb{E}\text{Res}(G_{(1)}) + \tau_u + \bar{L}/C$, $p_{1,5} = g_2/(2\tau + g_2 + g_3 + 2\tau + g_2 + g_3)$.

1,6 Packet is generated at ONU 1 during a cycle when ONU 1 has the shortest grant and is sending: $D_{1,6} = \mathbb{E}\text{Res}(G_{(3)}) + 2\tau + \rho \times \mathbb{E}\text{Res}(G_{(1)}) + \tau_u + \bar{L}/C$, $p_{1,6} = g_3/(2\tau + g_2 + g_3 + 2\tau + g_2 + g_3)$.

3,1 Packet is generated at ONU 3 during the 2τ period before a cycle when ONU 1 has the longest grant: $D_{3,1} = \tau_u + g_2 + g_3 + 2\tau + \rho \times \mathbb{E}\text{Res}(G_{(1)}) + \tau_u + \bar{L}/C$, $p_{3,1} = 2\tau/(2\tau + g_2 + g_3 + 2\tau + g_2 + g_3)$.

3,2 Packet is generated at ONU 3 when ONU 1 has the longest grant and ONU 2 is sending: $D_{3,2} = \mathbb{E}\text{Res}(G_{(2)}) + g_3 + 2\tau + \rho \times \mathbb{E}\text{Res}(G_{(1)}) + \tau_u + \bar{L}/C$, $p_{3,2} = g_2/(2\tau + g_2 + g_3 + 2\tau + g_2 + g_3)$.

3,3 Packet is generated at ONU 3 during a cycle when ONU 1 has the longest grant and ONU 3 is sending: $D_{3,3} = \mathbb{E}\text{Res}(G_{(3)}) + 2\tau + \rho \times \mathbb{E}\text{Res}(G_{(1)}) + \tau_u + \bar{L}/C$, $p_{3,3} = g_3/(2\tau + g_2 + g_3 + 2\tau + g_2 + g_3)$.

3,4 Packet is generated at ONU 3 during the 2τ period before ONU 1 has the shortest grant: $D_{3,4} = \tau_u + g_2 + g_3 + 2\tau + g_2 + \rho \times \mathbb{E}\text{Res}(G_{(3)}) + \tau_u + \bar{L}/C$, $p_{3,4} = 2\tau/(2\tau + g_2 + g_3 + 2\tau + g_2 + g_3)$.

3,5 Packet is generated at ONU 3 during a cycle when ONU 1 has the shortest grant and ONU 3 is sending: $D_{3,5} = \mathbb{E}\text{Res}(G_{(3)}) + g_2 + g_3 - g_1 + 2\tau + g_2 + \rho \times \mathbb{E}\text{Res}(G_{(3)}) + \tau_u + \bar{L}/C$, $p_{3,5} = g_1/(2\tau + g_2 + g_3 + 2\tau + g_2 + g_3)$.

3,6 Packet is generated at ONU 3 during a cycle when ONU 1 has the shortest grant, after ONU 3 has finished sending: $D_{3,6} = \mathbb{E}\text{Res}(G_{(2)} + G_{(3)} - G_{(1)}) + 2\tau + g_2 + g_3 + 2\tau + \rho \times \mathbb{E}\text{Res}(G_{(1)}) + \tau_u + \bar{L}/C$, $p_{3,6} = (g_2 + g_3 - g_1)/(2\tau + g_2 + g_3 + 2\tau + g_2 + g_3)$.

2,1 Packet is generated at ONU 2 during the 2τ time period before a cycle when ONU 1 has the longest grant: $D_{2,1} = \tau_u + g_2 + g_3 + 2\tau + \rho \times \mathbb{E}\text{Res}(G_{(2)}) + \tau_u + \bar{L}/C$, $p_{2,1} = 2\tau/(2\tau + g_2 + g_3 + 2\tau + g_2 + g_3)$.

2,2 Packet is generated at ONU 2 when ONU 1 has the longest grant and ONU 2 is sending: $D_{2,2} = \mathbb{E}\text{Res}(G_{(2)}) + g_3 + 2\tau + \rho \times \mathbb{E}\text{Res}(G_{(2)}) + \tau_u + \bar{L}/C$, $p_{2,2} = g_2/(2\tau + g_2 + g_3 + 2\tau + g_2 + g_3)$.

2,3 Packet is generated at ONU 2 during a cycle when ONU 1 has the longest grant and ONU 3 is sending: $D_{2,3} = \mathbb{E}\text{Res}(G_{(3)}) + 2\tau + g_2 + g_3 + 2\tau + \rho \times \mathbb{E}\text{Res}(G_{(2)}) + \tau_u + \bar{L}/C$, $p_{2,3} = g_3/(2\tau + g_2 + g_3 + 2\tau + g_2 + g_3)$.

2,4 Packet is generated at ONU 2 during the 2τ period before ONU 1 has the shortest grant: $D_{2,4} = \tau_u + g_2 + g_3 + 2\tau + \rho \times \text{ERes}(G_{(2)}) + \tau_u + \bar{L}/C$, $p_{2,4} = 2\tau / (2\tau + g_2 + g_3 + 2\tau + g_2 + g_3)$.

2,5 Packet is generated at ONU 2 during a cycle when ONU 1 has the shortest grant and ONU 2 is sending: $D_{2,5} = \text{ERes}(G_{(2)}) + g_3 + 2\tau + \rho \times \text{ERes}(G_{(2)}) + \tau_u + \bar{L}/C$, $p_{2,5} = g_2 / (2\tau + g_2 + g_3 + 2\tau + g_2 + g_3)$.

2,6 Packet is generated at ONU 2 during a cycle when ONU 1 has the shortest grant and ONU 2 is sending: $D_{2,6} = \text{ERes}(G_{(3)}) + 2\tau + g_2 + g_3 + 2\tau + \rho \times \text{ERes}(G_{(2)}) + \tau_u + \bar{L}/C$, $p_{2,6} = g_3 / (2\tau + g_2 + g_3 + 2\tau + g_2 + g_3)$.

ACKNOWLEDGMENTS

We are grateful to Dr. Michael McGarry of The University of Akron, Jason Ferguson of ADTRAN, and Stephen Charnicki of Arizona State University for assistance with the numerical work and simulations. This work was supported by the DFG Research Center MATHEON "Mathematics for key technologies" in Berlin, Germany.

REFERENCES

- [1] C. Assi, Y. Ye, S. Dixit, and M. Ali, "Dynamic bandwidth allocation for quality-of-service over Ethernet PONs," *IEEE J. Sel. Areas Commun.*, vol. 21, no. 9, pp. 1467–1477, Nov. 2003.
- [2] C. Foh, L. Andrew, E. Wong, and M. Zukerman, "FULL-RCMA: a high utilization EPON," *IEEE J. Sel. Areas Commun.*, vol. 22, no. 8, pp. 1514–1524, Oct. 2004.
- [3] G. Kramer, B. Mukherjee, and G. Pesavento, "Ethernet PON (ePON): design and analysis of an optical access network," *Photonic Network Commun.*, vol. 3, no. 3, pp. 307–319, July 2001.
- [4] M. Ma, Y. Zhu, and T. Cheng, "A bandwidth guaranteed polling MAC protocol for Ethernet passive optical networks," in *Proc. IEEE INFOCOM*, San Francisco, CA, March 2003, vol. 1, pp. 22–31.
- [5] R. Mastrodonato and G. Paltenghi, "Analysis of a bandwidth allocation protocol for Ethernet passive optical networks (EPONs)," in *Proc. of IEEE Int. Conf. on Transparent Optical Networks*, 2005, pp. 241–244.
- [6] M. McGarry, M. Maier, and M. Reisslein, "Ethernet PONs: a survey of dynamic bandwidth allocation (DBA) algorithms," *IEEE Commun. Mag.*, vol. 42, no. 8, pp. S8–S15, Aug. 2004.
- [7] H. Naser and H. Mouftah, "A joint-ONU interval-based dynamic scheduling algorithm for Ethernet passive optical networks," *IEEE/ACM Trans. Netw.*, vol. 14, no. 4, pp. 889–899, Aug. 2006.
- [8] A. Shami, X. Bai, C. Assi, and N. Ghani, "Jitter performance in Ethernet passive optical networks," *J. Lightwave Technol.*, vol. 23, no. 4, pp. 1745–1753, Apr. 2005.
- [9] A. Shami, X. Bai, N. Ghani, C. Assi, and H. Mouftah, "QoS control schemes for two-stage Ethernet passive optical access networks," *IEEE J. Sel. Areas Commun.*, vol. 23, no. 8, pp. 1467–1478, Aug. 2005.
- [10] A. Sierra and S. V. Kartalopoulos, "Evaluation of two prevalent EPON networks using simulation methods," in *Proc. of the Advanced Int. Conf. on Telecommunications and Int. Conf. on Internet and Web Applications and Services*, 2006, pp. 48–53.
- [11] J. Zheng and H. Mouftah, "Media access control for Ethernet passive optical networks: an overview," *IEEE Commun. Mag.*, vol. 43, no. 2, pp. 145–150, Feb. 2005.
- [12] J. Zheng, "Efficient bandwidth allocation algorithm for Ethernet passive optical networks," *IEE Proc.-Commun.*, vol. 153, no. 3, pp. 464–468, June 2006.
- [13] F. An, K. Kim, D. Gutierrez, S. Yam, E. Hu, K. Shrikhande, and L. Kazovsky, "SUCCESS: a next-generation hybrid WDM/TDM optical access network architecture," *J. Lightwave Technol.*, vol. 22, no. 11, pp. 2557–2569, Nov. 2004.
- [14] A. Banerjee, Y. Park, F. Clarke, H. Song, S. Yang, G. Kramer, K. Kim, and B. Mukherjee, "Wavelength-division-multiplexed passive optical network (WDM-PON) technologies for broadband access: a review," *J. Opt. Netw.*, vol. 4, no. 1, pp. 737–758, Nov. 2005.
- [15] W.-R. Chang, H.-T. Lin, S.-J. Hong, and C.-L. Lai, "A novel WDM EPON architecture with wavelength spatial reuse in high-speed access networks," in *Proc. of the 15th IEEE Int. Conf. on Networks (ICON)*, 2007, pp. 155–160.
- [16] A. Dhaini, C. Assi, M. Maier, and A. Shami, "Dynamic wavelength and bandwidth allocation in hybrid TDM/WDM EPON networks," *J. Lightwave Technol.*, vol. 25, no. 1, pp. 277–286, Jan. 2007.
- [17] K. Kwong, D. Harle, and I. Andonovic, "Dynamic bandwidth allocation algorithm for differentiated services over WDM EPONs," in *Proc. Ninth Int. Conf. on Communications Systems*, Sept. 2004, pp. 116–120.
- [18] K. Kim, D. Gutierrez, F. An, and L. Kazovsky, "Design and performance analysis of scheduling algorithms for WDM-PON under SUCCESS-HPON architecture," *J. Lightwave Technol.*, vol. 23, no. 11, pp. 3716–3731, Nov. 2005.
- [19] M. McGarry, M. Maier, and M. Reisslein, "WDM Ethernet passive optical networks," *IEEE Commun. Mag.*, vol. 44, no. 2, pp. S18–S25, Feb. 2006.
- [20] M. McGarry, M. Reisslein, M. Maier, and A. Keha, "Bandwidth management for WDM EPONs," *J. Opt. Netw.*, vol. 5, no. 9, pp. 637–654, Sept. 2006.
- [21] C. Xiao, B. Bing, and G. Chang, "An efficient MAC protocol with pre-allocation for high-speed WDM passive optical networks," in *Proc. of IEEE Infocom*, Miami, FL, March 2005.
- [22] M. McGarry, M. Reisslein, C. Colbourn, M. Maier, F. Aurzada, and M. Scheutzw, "Just-in-time scheduling for multichannel EPONs," *J. Lightwave Technol.*, vol. 26, no. 10, pp. 1204–1216, May 2008.
- [23] J. Zheng and H. Mouftah, "A survey of dynamic bandwidth allocation algorithms for Ethernet passive optical networks," *Opt. Switching Networking*, vol. 6, no. 3, pp. 151–162, July 2009.
- [24] X. Bai, C. Assi, and A. Shami, "On the fairness of dynamic bandwidth allocation schemes in Ethernet passive optical networks," *Comput. Commun.*, vol. 29, no. 11, pp. 2125–2135, July 2006.
- [25] N. Kim, H. Yun, and M. Kang, "Analysis of effect of load-based excess bandwidth reservation on performances of differentiated services in E-PON," *IET Commun.*, vol. 1, no. 3, pp. 382–390, Jan. 2007.
- [26] F. Melo Pereira, N. L. S. Fonseca, and D. S. Arantes, "A fair scheduling discipline for Ethernet passive optical networks," *Comput. Netw.*, vol. 53, no. 11, pp. 1859–1878, July 2009.
- [27] H. Takagi, *Analysis of Polling Systems*. MIT Press, 1986.
- [28] H. Takagi, "Analysis and application of polling models," in *Performance Evaluation: Origins and Directions, Lecture Notes in Computer Science, Vol. 1769*, G. Haring, C. Lindemann, and M. Reiser, eds. Springer, 2000, pp. 423–442.
- [29] G. Kramer, B. Mukherjee, and G. Pesavento, "Interleaved polling with adaptive cycle time (IPACT): a dynamic bandwidth distribution scheme in an optical access network," *Photonic Network Commun.*, vol. 4, no. 1, pp. 89–107, Jan. 2002.

- [30] G. Kramer, B. Mukherjee, and G. Pesavento, "IPACT: a dynamic protocol for an Ethernet PON (EPON)," *IEEE Commun. Mag.*, vol. 40, no. 2, pp. 74–80, Feb. 2002.
- [31] S. Bhatia and R. Bartos, "Closed-form expression for the collision probability in the IEEE Ethernet passive optical network registration scheme," *J. Opt. Netw.*, vol. 5, no. 1, pp. 1–14, Jan. 2005.
- [32] T. Holmberg, "Analysis of EPONs under the static priority scheduling scheme with fixed transmission times," in *Proc. IEEE Conf. on Next Generation Internet Design and Engineering (NGI)*, Apr. 2006, pp. 192–199.
- [33] B. Lannoo, L. Verslegers, D. Colle, M. Pickavet, M. Gagnaire, and P. Demeester, "Analytical model for the IPACT dynamic bandwidth allocation algorithm in EPONs," *J. Opt. Netw.*, vol. 6, no. 6, pp. 677–688, June 2007.
- [34] S. Bhatia, D. Garbuzov, and R. Bartos, "Analysis of the gated IPACT scheme for EPONs," in *Proc. IEEE ICC*, June 2006, pp. 2693–2698.
- [35] X. Bai, A. Shami, and Y. Ye, "Delay analysis of Ethernet passive optical networks with quasi-leaved polling and gated service scheme," in *Proc. of Second Int. Conf. on Access Networks*, 2007, pp. 1–8.
- [36] F. Aurzada, M. Scheutzow, M. Herzog, M. Maier, and M. Reisslein, "Delay analysis of Ethernet passive optical networks with gated service," *J. Opt. Netw.*, vol. 7, no. 1, pp. 25–41, Jan. 2008.
- [37] M. T. Ngo, A. Gravey, and D. Bhadauria, "A mean value analysis approach for evaluating the performance of EPON with gated IPACT," in *Proc. of Int. Conf. on Optical Network Design and Modeling (ONDM)*, 2008, pp. 1–6.
- [38] Y. Luo and N. Ansari, "Bandwidth management and delay control over EPONs," in *Proc. IEEE Workshop on High Performance Switching and Routing (HPSR)*, May 2005, pp. 457–461.
- [39] Y. Luo and N. Ansari, "Dynamic upstream bandwidth allocation over Ethernet PONs," in *Proc. IEEE ICC*, May 2005, pp. 1853–1857.
- [40] Y. Zhu and M. Ma, "IPACT with grant estimation (IPACT-GE) scheme for Ethernet passive optical networks," *J. Lightwave Technol.*, vol. 26, no. 14, pp. 2055–2063, July 2008.
- [41] K. Tanaka, K. Ohara, N. Miyazaki, and N. Edagawa, "Performance analysis of Ethernet PON system accommodating 64 ONUs," *J. Opt. Netw.*, vol. 6, no. 5, pp. 559–566, May 2007.
- [42] M. Hajduczenia, H. J. A. da Silva, and P. P. Monteiro, "EPON versus APON and GPON: a detailed performance comparison," *J. Opt. Netw.*, vol. 5, no. 4, pp. 298–319, Apr. 2006.
- [43] J. Vardakas, V. Vassilakis, and M. Logothetis, "Blocking analysis for priority classes in hybrid WDM-OCDMA passive optical networks," in *Proc. of Fifth Advanced Int. Conf. on Telecommunications (AICT)*, 2009, pp. 389–394.
- [44] W.-R. Chang, "Research and design of system architectures and communication protocols for next-generation optical networks," Ph.D. dissertation, National Cheng Kung University, Tainan, Taiwan, 2008.
- [45] C. G. Park, D. H. Han, and K. W. Rim, "Packet delay analysis of symmetric gated polling system for DBA scheme in an EPON," *Telecommun. Syst.*, vol. 30, no. 1–3, pp. 13–34, Nov. 2005.
- [46] I. Eliazar, "Gated polling systems with Levy inflow and interdependent switchover times: a dynamical-systems approach," *Queueing Syst.*, vol. 49, no. 1, pp. 49–72, Jan. 2005.
- [47] I. Eliazar, "From polling to snowplowing," *Queueing Syst.*, vol. 51, no. 1–2, pp. 115–133, Oct. 2005.
- [48] R. Groeneveld and E. Altman, "Analysis of alternating-priority queueing models with (cross) correlated switchover times," *Queueing Syst.*, vol. 51, no. 3–4, pp. 199–247, Dec. 2005.
- [49] H. Levy and M. Sidi, "Polling systems with correlated arrivals," in *Proc. of IEEE Infocom*, Apr. 1989, pp. 907–913.
- [50] T. Lee and J. Sunjaya, "Exact analysis of asymmetric random polling systems with single buffers and correlated input process," *Queueing Syst.*, vol. 23, no. 1–4, pp. 131–156, Mar. 1996.
- [51] M. M. Srinivasan, S.-C. Niu, and R. B. Cooper, "Relating polling models with zero and nonzero switchover times," *Queueing Syst.*, vol. 19, no. 1–2, pp. 149–168, Mar. 1995.
- [52] F. Effenberger, D. Clearly, O. Haran, G. Kramer, R. D. Li, M. Oron, and T. Pfeiffer, "An introduction to PON technologies," *IEEE Commun. Mag.*, vol. 45, no. 3, pp. S17–S25, Mar. 2007.
- [53] L. Meng, C. Assi, M. Maier, and A. Dhaini, "Resource management in STARGATE-based Ethernet passive optical networks (SG-EPONs)," *J. Opt. Commun. Netw.*, vol. 1, no. 4, pp. 279–293, Sept. 2009.
- [54] L. Meng, J. El-Najjar, H. Alazemi, and C. Assi, "A joint transmission grant scheduling and wavelength assignment in multichannel SG-EPON," *J. Lightwave Technol.*, vol. 27, no. 21, pp. 4781–4792, Nov. 2009.
- [55] K. Grobe and J.-P. Elbers, "PON in adolescence: from TDMA to WDM-PON," *IEEE Commun. Mag.*, vol. 46, no. 1, pp. 26–34, Jan. 2008.
- [56] M. Maier, "WDM passive optical networks and beyond: the road ahead [invited]," *J. Opt. Commun. Netw.*, vol. 1, no. 4, pp. C1–C16, Sept. 2009.
- [57] B. Skubic, J. Chen, J. Ahmed, L. Wosinska, and B. Mukherjee, "A comparison of dynamic bandwidth allocation for EPON, GPON, and next-generation TDM PON," *IEEE Commun. Mag.*, vol. 47, no. 3, pp. S40–S48, Mar. 2009.
- [58] F. Aurzada, M. Scheutzow, M. Reisslein, N. Ghazisaidi, and M. Maier, "Capacity and delay analysis of next-generation passive optical networks (NG-PONs)," Technical Report, Arizona State University, Electrical Eng., 2009, http://mre.faculty.asu/NG_PONs.pdf.
- [59] M. Pinedo, *Scheduling: Theory, Algorithms, and Systems*, 3rd ed., Springer, 2008.
- [60] G. Dan, V. Fodor, and G. Karlsson, "On the effects of the packet size distribution on FEC performance," *Comput. Netw.*, vol. 50, no. 8, pp. 1023–1192, June 2006.
- [61] R. Sinha, C. Papadopoulos, and J. Heidemann, "Internet packet size distributions: some observations," Oct. 2005, <http://network.usc.edu/~rsinha/pkt-sizes/>.
- [62] G. Kramer, "Generator of self-similar traffic," 2001, <http://wwwcsif.cs.ucdavis.edu/kramer/>.
- [63] M. S. Taqqu, W. Willinger, and R. Sherman, "Proof of fundamental result in self-similar traffic modeling," *Comput. Commun. Rev.*, vol. 27, no. 2, pp. 5–23, Apr. 1997.
- [64] X. Fang and M. Veeraraghavan, "A hybrid network architecture for file transfers," *IEEE Trans. Parallel Distrib. Syst.*, vol. 20, no. 12, pp. 1714–1725, Dec. 2009.